The potential role and rationale for treatment of heart failure with sodium-glucose co-transporter 2 inhibitors

Butler, Javed; Hamo, Carine E; Filippatos, Gerasimos; Pocock, Stuart J; Bernstein, Richard A; Brueckmann, Martina; Cheung, Alfred K; George, Jyothis T; Green, Jennifer B; Januzzi, James L; Kaul, Sanjay; Lam, Carolyn S P; Lip, Gregory Y H; Marx, Nikolaus; McCullough, Peter A; Mehta, Cyrus R; Ponikowski, Piotr; Rosenstock, Julio; Sattar, Naveed; Salsali, Afshin; Scirica, Benjamin M; Shah, Sanjiv J; Tsutsui, Hiroyuki; Verma, Subodh; Wanner, Christoph; Woerle, Hans-Juergan; Zannad, Faiez; Anker, Stefan D; EMPEROR Trials Program

Published in:
European Journal of Heart Failure

DOI (link to publication from Publisher):
10.1002/ejhf.933

Publication date:
2017

Document Version
Accepted author manuscript, peer reviewed version

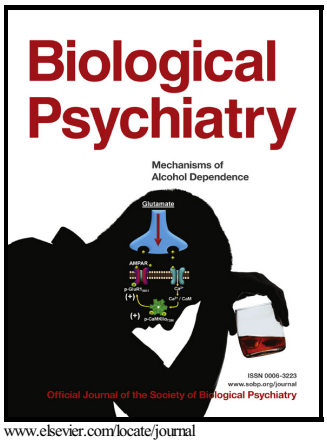

www.elsevier.com/locate/journal

The schizophrenia associated *BRD1* gene regulates behavior, neurotransmission, and expression of schizophrenia risk enriched gene sets in miceBRD1 in schizophrenia, behavior, and neurobiology

Per Qvist, Jane Hvarregaard Christensen, Irina Vardya, Anto Praveen Rajkumar, Arne Mørk, Veerle Paternoster, Ernst-Martin Füchtbauer, Jonatan Pallesen, Tue Fryland, Mads Dyrvig, Mads Engel Hauberg, Birgitte Lundsberg, Kim Fejgin, Mette Nyegaard, Kimmo Jensen, Jens Randel Nyengaard, Ole Mors, Michael Didriksen, Anders Dupont Børglum

PII: S0006-3223(16)32780-9
DOI: http://dx.doi.org/10.1016/j.biopsych.2016.08.037
Reference: BPS12990

To appear in: *Biological Psychiatry*

Received date: 5 February 2016
Revised date: 18 August 2016
Accepted date: 29 August 2016

Cite this article as: Per Qvist, Jane Hvarregaard Christensen, Irina Vardya, Anto Praveen Rajkumar, Arne Mørk, Veerle Paternoster, Ernst-Martin Füchtbauer, Jonatan Pallesen, Tue Fryland, Mads Dyrvig, Mads Engel Hauberg, Birgitte Lundsberg, Kim Fejgin, Mette Nyegaard, Kimmo Jensen, Jens Randel Nyengaard, Ole Mors, Michael Didriksen and Anders Dupont Børglum, The schizophrenia associated *BRD1* gene regulates behavior, neurotransmission, and expression of schizophrenia risk enriched gene sets in miceBRD1 in schizophrenia, behavior, and neurobiology, *Biological Psychiatry,* http://dx.doi.org/10.1016/j.biopsych.2016.08.037

Title: THE SCHIZOPHRENIA ASSOCIATED *BRD1* GENE REGULATES BEHAVIOR, NEUROTRANSMISSION, AND EXPRESSION OF SCHIZOPHRENIA RISK ENRICHED GENE SETS IN MICE

Short title: BRD1 in schizophrenia, behavior, and neurobiology

Per Qvist[1-4†], Jane Hvarregaard Christensen[1-3†], Irina Vardya[1], Anto Praveen Rajkumar[1-3], Arne Mørk[4], Veerle Paternoster[1-3], Ernst-Martin Füchtbauer[5], Jonatan Pallesen[1-3], Tue Fryland[1-3], Mads Dyrvig[1,6], Mads Engel Hauberg[1-3], Birgitte Lundsberg[1], Kim Fejgin[4], Mette Nyegaard[1-3], Kimmo Jensen[1], Jens Randel Nyengaard[7], Ole Mors[2,3,8], Michael Didriksen[4] and Anders Dupont Børglum[1-3*]

[1]Department of Biomedicine, Aarhus University, 8000 Aarhus C, Denmark.
[2]*i*PSYCH, The Lundbeck Foundation Initiative for Integrative Psychiatric Research, 8000 Aarhus C, Denmark.
[3]*i*SEQ, Centre for Integrative Sequencing, Aarhus University, 8000 Aarhus C, Denmark.
[4]H. Lundbeck A/S, Synaptic Transmission, 2500 Valby, Denmark.
[5]Department of Molecular Biology and Genetics, Aarhus University, 8000 Aarhus C, Denmark.
[6]Department of Health Science and Technology, Aalborg University, 9100 Aalborg, Denmark.
[7]Stereology and EM Laboratory, Centre for Stochastic Geometry and Advanced Bioimaging, Aarhus University, 8000 Aarhus C, Denmark.
[8]Psychosis Research Unit, Aarhus University Hospital, 8240 Risskov, Denmark.

[*]To whom correspondence should be addressed:
Professor Anders Dupont Børglum, MD, PhD
Department of Biomedicine, Aarhus University
Bartholins Allé 6
DK-8000 Aarhus C
Denmark
Tel: +45 87 16 77 68
FAX: +45 86 12 31 73
E-mail: ANDERS@BIOMED.AU.DK

[†] These authors contributed equally to the work

Key words: BRD1, knockout mouse, schizophrenia, behavior, electrophysiology, RNAseq, monoaminergic neurotransmission, cyclic AMP response element-binding protein (CREB), DARPP32 signaling

Abstract:

Background: The schizophrenia-associated *BRD1* gene encodes a transcriptional regulator whose comprehensive chromatin interactome is enriched with schizophrenia risk genes. However, the biology underlying the disease association of *BRD1* remains speculative.

Methods: This study assessed the transcriptional drive of a schizophrenia-associated *BRD1* risk variant *in vitro*. Accordingly, to examine the effects of reduced *Brd1* expression, we generated a genetically modified *Brd1*$^{+/-}$ mouse and subjected it to behavioral, electrophysiological, molecular, and integrative genomic analyses with focus on schizophrenia-relevant parameters.

Results: *Brd1*$^{+/-}$ mice displayed cerebral histone H3K14 hypo-acetylation and a broad range of behavioral changes with translational relevance to schizophrenia. These behaviors were accompanied by striatal dopamine/serotonin abnormalities and cortical excitation-inhibition imbalances involving loss of *parvalbumin* immunoreactive interneurons. RNAseq analyses of cortical and striatal micropunches from *Brd1*$^{+/-}$ and wild-type mice revealed differential expression of genes enriched for schizophrenia risk including several schizophrenia GWAS risk genes (e.g. calcium channel subunits (*Cacna1c* and *Cacnb2*), cholinergic muscarinic receptor 4 (C*hrm4*), dopamine receptor D2 (*Drd2*), and transcription factor 4 (*Tcf4*)). Integrative analyses further found differentially expressed genes to cluster in functional networks and canonical pathways associated with mental illness and molecular signaling processes (e.g. glutamatergic, monaminergic, calcium, cAMP, DARPP-32, and CREB signaling).

Conclusions: Our study bridges the gap between genetic association and pathogenic effects and yields novel insights into the unfolding molecular changes in the brain of a new schizophrenia model that incorporates genetic risk at three levels: allelic, chromatin interactomic, and brain transcriptomic.

Introduction

Schizophrenia is a common and severe mental disorder. It is highly heritable with a notably polygenic genetic architecture comprising thousands of risk variants (1; 2). The distal part of chromosome 22q has long been implicated with schizophrenia (3; 4) and a susceptibility locus at 22q13.3 has been identified in the isolated population of the Faroe Islands (5). The *BRD1* gene, which is located within this locus, has repeatedly been associated with schizophrenia in large Caucasian case-control samples (6; 7) and the *BRD1* promoter SNP rs138880 was recently identified as the most significantly associated variant in a large schizophrenia GWAS meta-analysis (11,185 cases and 10,768 controls) and family-based replication study (6,298 individuals including 3,286 cases) (8). Although the *BRD1* locus falls short of genome-wide significance in the Psychiatric Genomics Consortium (PGC) schizophrenia mega-GWASs using traditional statistical methods (p=4.38E-05 in PGC1 (1) and p=3.31E-07 in PGC2 (2)), the locus is found genome-wide significant and predicted to be highly replicable when applying an Empirical Bayes statistical approach already in the PGC1 dataset (9).

BRD1 encodes the bromodomain-containing protein 1 (BRD1) which has been identified in complexes possessing acetyltransferase activity towards histone H3 (10) – in particular H3K14 (11). In cell lines, BRD1 is found attached to genomic regions, primarily close to transcription start sites, and it has been demonstrated to influence the expression of large gene sets (11; 12). Pointing to an involvement of *BRD1* as a regulatory hub gene in brain development and susceptibility to mental illness, the BRD1 chromatin interactome is significantly enriched for schizophrenia risk – and in particular with genes acting in signaling pathways important during neurodevelopment (12). In line with this, BRD1 is essential during embryogenesis as inactivation of both alleles of *Brd1* in mice leads to compromised eye development, neural tube closure, and a lethal maturation defect in

embryonic hematopoiesis (11). Although its cortical expression level peaks during intrauterine development (13), *BRD1* remains widely and abundantly expressed in the adult mammalian central nervous system (6; 14) and a role in the postnatal brain has been indicated by its differential regulation in various brain regions in rats upon both electroconvulsive seizures (15) and chronic restraint stress (16). Combined, current data suggest that BRD1 is important for both pre- and postnatal transcriptional regulation in the brain and could contribute to schizophrenia etiopathology by influencing histone modification and thereby the chromatin state around multiple schizophrenia risk genes.

In the present study, we show that human *BRD1* promoter risk alleles correlate with reduced *BRD1* mRNA and reduced transcriptional drive. We demonstrate that genetically engineered mice (*Brd1*$^{+/-}$ mice) with reduced *Brd1* expression and cerebral H3K14 hypoacetylation recapitulate key features of schizophrenia symptomatology and neurochemistry. Through a range of molecular, cellular, and bioinformatic investigations, including transcriptome profiling of selected brain regions, we provide novel insight into the biological changes that underlie the phenotypes and suggest links relevant to schizophrenia etiopathology.

Methods and Materials

eQTL analysis

cis-eQTL analysis was performed on the HapMap phase III dataset for CEU (n=55) individuals including SNPs located within 35 kb upstream and 10 kb downstream from the transcriptional start site of BRD1. Cis-eQTL effects of SNPs in LD with risk alleles were similarly assessed in the Blood eQTL browser (http://genenetwork.nl/bloodeqtlbrowser/) (17), BrainCloud Web site (http://braincloud.jhmi.edu/downloads.htm) and GTEx V6 (http://www.gtexportal.org/home/). For further details, see **Supplemental Methods and Materials**.

Dual luciferase assay of BRD1 promoter fragments

Genomic DNA from two in-house control subjects homozygous for the A or C allele of the rs138880 SNP was used as templates to PCR amplify a 1031 bp region of the promoter potentially driving the transcription of the short exon 7 variant of *BRD1*. Both subjects provided written, informed consent for participation, and approval was obtained from local ethics committees. See **Supplemental Methods and Materials** for details.

Animals

A mouse line heterozygous for a targeted deletion within the *Brd1* gene, *Brd1*$^{tm1569.2Arte}$ (*Brd1*$^{+/-}$) was generated by TaconicArtemis GmbH (Cologne, Germany) using a targeting vector (pBrd1 Final cl 1 (UP0257)) with loxP sites flanking exon 3-5 of the *Brd1* gene. For further details, see **Supplemental Methods and Materials**. Animal experiments were performed according to institutional and national regulations.

Quantitative reverse transcription-PCR and Western blotting

Detailed information on quantitative reverse transcription-PCR and Western blotting procedures can be found in **Supplemental Methods and Materials**.

Morphological analysis of embryos and general assessment of health, physiology, neurology, and motor coordination

Details on morphological analysis of embryos as well as growth curves, organ and bone measures, hematology, functional observation battery, acute pain response, hidden food retrieval test for olfaction, rotarod, balance beam walking, and footprinting on adolescent mice can all be viewed in **Supplemental Methods and Materials**.

Behavioral phenotyping

Detailed description of social interaction, three-chamber sociability and preference for novelty test, spontaneous alternation, continuous alternation, and contextual fear conditioning, associative memory retrieval, prepulse inhibition (PPI), spontaneous- and drug-induced hyperactivity, PTZ-induced seizures and drugs used in testing can all be found in **Supplemental Methods and Materials.**

Quantification of neurotransmitters

Mice were sacrificed by cervical dislocation and striatal tissue was collected by free-hand dissection and processed for HPLC analyses. For details on HPLC protocols, see **Supplemental Methods and Materials**.

Brain slice electrophysiology

Whole-cell patch-clamp recordings of $GABA_A$-receptor-mediated currents were performed in acute coronal brain slices of 7-8 weeks old male mice (number of mice (*n*) in **Tables S5**). For details see **Supplemental Methods and Materials**.

RNAseq analysis on tissue micropunches

Briefly, brains from adolescent mice were snap frozen in 2-methylbutane and sectioned (1 mm) coronally at -20°C. aCC and striatum (caudate nucleus) were identified (18) and punched by a needle (1 mm diameter). RNAseq experiments and analyses were performed as previously described (19). For details and validation of DEGs, see **Supplemental Methods and Materials**.

Immunohistochemistry and stereology

Brains from 8 weeks old formaldehyde perfused mice were moulded in Tissue-Tek® (Sakura, Tokyo, Japan). 40 µm coronal sections containing aCC (Bregma 1.5 mm. to 0.5 mm.) were cut at -20°C using a MICROM HM355 cryostat and immunohistochemically stained with an antibody directed against Parvalbumin (Pvalb). For more details and description of stereological measures see **Supplemental Methods and Materials**.

Enrichment analysis of DEGs

Gene set analysis was performed with MAGMA (20) using default settings, based on summary statistics from the PGC2 schizophrenia GWAS (2) and other publicly available GWASs while excluding the MHC region and imputed SNPs with info score < 0.8. The gene annotation files consisted of lists of genes detected in aCC, striatum, and the two regions combined. See **Supplemental Methods and Materials** for details.

Analysis of overlap between DEGs and genes located in schizophrenia GWAS risk loci

The significance of overlap between the set of DEGs and genes in schizophrenia GWAS risk loci, as defined by others (2), was analyzed using permutation analysis based on the combined transcripts detected in striatum and in aCC (n=42,198) for which human homologous genes exist (n=20,958). In each permutation a gene set was sampled with the same number of genes as the DEG set, and containing genes of similar sizes as the genes in the DEG set. The *p* value of the significance of the

overlap was estimated as the number of permuted gene sets that contained equally many or more genes present in schizophrenia GWAS loci as the set of nominally significant DEGs, divided by the total number of permutations.

Statistical analysis

STATA 12.1 (StataCorp LP, Texas, U.S.) and GraphPad Prism 5.01 software (GraphPad software, San Diego, CA, USA) was used for statistical analysis of animal data and OriginPro9 (OriginLab Corporation, Northampton, MA, U.S.) for electrophysiological recordings (see respective result sections and figure legends for details).

Results

Correlation between BRD1 risk alleles and BRD1 expression

Due to the location of the rs138880 SNP in a putative *BRD1* promoter binding site for transcriptional repressor HES1 (6), we assessed the association between the SNP and *BRD1* expression in a cis-eQTL analysis using a publically available dataset with expression phenotypes of B lymphoblastoid cell lines established from HapMap3 individuals (21). We found that carriers of the rs138880 risk allele (C allele) expressed significantly less *BRD1* mRNA than non-carriers among individuals of European ancestry (**Figure 1A**, $p<0.05$ and **Table S1**). SNPs in high LD with rs138880 were likewise correlated with *BRD1* mRNA levels, including all reported SNPs in *BRD1* that have shown association with schizophrenia (6–8; 22) (**Figure S1** and **Table S1**). The same effect was seen for SNPs in the haploblock in a larger blood eQTL dataset (5,311 individuals, p=9.0E-07, Z-score =-5.2 for the most significant SNP) (17) and similarly in a relatively small brain eQTL dataset for a SNP (rs7410537) in strong LD with rs138880 (**Figure 1B**, 112 individuals, p=0.08) (13) whereas no significant *BRD1* cis-eQTLs were found in the GTEx database (23).

To investigate whether particularly the rs138880 alleles have different transcriptional drive, we cloned the promoter region harboring either the A or C allele of rs138880 (and otherwise being 100% identical) into a luciferase reporter vector (**Figure 1C**). Four independent transfections of these vectors into mouse neuroblastoma Neuro2A cells (with co-transfection of a pRL-TK vector for normalization) revealed that transcriptional drive was significantly lower for the fragment containing the risk C allele (**Figure 1C** and **Figure S2**).

Generation and basic characterization of heterozygous Brd1$^{+/-}$ mice

In order to examine the behavioral and underlying neurophysiological and molecular consequences of reduced *Brd1* expression, we generated a strain of heterozygous *Brd1*$^{tm1569.2Arte}$ (*Brd1*$^{+/-}$) mice carrying a deletion of exon 3-5 of the *Brd1* gene (**Figure 1D** and **Figure S3A**). The deletion is expected to target all annotated transcript variants of the gene by introducing a premature stop codon in exon 6. *Brd1* mRNA expression was reduced to approximately 50% in *Brd1*$^{+/-}$ mice compared to wild type (WT) mice in all tissues examined (**Figure 1E** and **Figure S3B-E**). This was substantiated by Western blotting analysis of whole brain extracts, showing a reduction in immunoreactive BRD1 protein ranging between 30-48% (**Figure 1F** and **Figure S3F**). *Brd1*$^{+/-}$ mice were healthy and overall physiologically indistinguishable from WT mice (**Figure S4 and Supplemental results**).

In line with BRD1's role as a transcriptional regulator in the brain and in accordance with what has previously been reported in erythroblasts derived from BRD1 depleted mice (11), we found that global cerebral H3K14 acetylation was reduced by ~19% in male *Brd1*$^{+/-}$ mice (**Figure 1G**, $p<0.05$).

Behavioral assessment of heterozygous Brd1$^{+/-}$ mice

Given the genetic association of *BRD1* with schizophrenia and the enrichment of schizophrenia risk genes in its chromatin interactome, we assessed the performance of *Brd1*$^{+/-}$ male mice in a comprehensive panel of behavioral tasks (**Table 1**) designed to evaluate whether reduced *Brd1* expression elicits behavioral changes with translational relevance to schizophrenia symptomatology (24–27) - either at baseline or in response to psychotomimetic drugs.

Social behavior, cognition and information processing

To investigate behaviors with face validity to negative symptoms in schizophrenia, we observed the social behavior of *Brd1*$^{+/-}$ mice in a test for direct social interaction. *Brd1*$^{+/-}$ mice did not differ from

WT littermates on total time spent investigating an unfamiliar mouse of same genotype (**Figure 2A**). However, they spent less time engaged in passive interactions (**Figure 2A**, $p<0.05$), aggressive behavior was almost exclusively displayed by *Brd1*$^{+/-}$ mice (**Figure 2A**, $p<0.05$), and they showed a significant increase in latency to first social interaction (**Figure 2B**, $p<0.01$).
In a test for sociability and preference for social novelty, *Brd1*$^{+/-}$ mice lacked the preference for social stimuli in the form of prioritized exploration of a real mouse over a toy mouse (**Figure 2C**, $p<0.001$). They, however, acknowledged formerly introduced mice by displaying preferential exploration of novel mice over familiar mice to the same degree as did WT mice (**Figure 2D**). In an extension of this test, we exposed target mice to the same "novel" mouse (now familiar) and a new novel mouse a week after the first test to assess long-term social recognition memory. In this setting, *Brd1*$^{+/-}$ mice displayed significantly less preference investigating the new novel mice compared to WT mice (**Figure 2E**, $p<0.05$).

In the fear conditioning test for associative learning and contextual long term memory, levels of pre-training (basal) freezing did not differ between genotypes (**Figure 2F**). However, *Brd1*$^{+/-}$ mice spent significantly less time freezing compared to WT mice during the acquisition phase (**Figure 2F**, genotype effect, $F_{1,20}=8.142$, $p<0.01$) and following post-acquisition recording (**Figure 2F**, $p<0.05$), whereas motor activity did not differ between the groups (**Figure S5J**). Supportive of a deficit in long term memory, as indicated in the test for social recognition memory, *Brd1*$^{+/-}$ mice displayed less time freezing than WT mice when re-introduced to the context box 3 days after acquisition (**Figure 2G**, $p<0.01$), more prominently 7 days after acquisition (**Figure 2G**, $p<0.001$) compared to freezing 1 hour after acquisition, and with a clear decline of freezing behavior in *Brd1*$^{+/-}$ mice over time (**Figure 2G**, $p<0.05$). In tests for working memory, *Brd1*$^{+/-}$ mice performed significantly worse than their WT littermates when treated with a low dose of the NMDA receptor antagonist, phencyclidine (PCP, 1.3 mg/kg) (**Figure S5K-M and Supplemental results**).

Sensorimotor gating, as measured by prepulse inhibition of the acoustic startle response (PPI), is commonly decreased in individuals with schizophrenia indicating an impaired pre-attentive information processing (28; 29). This can be readily assessed in rodents (30; 31) with or without the administration of psychotomimetics (32).

Baseline PPI response was similar in *Brd1*$^{+/-}$ and WT mice (**Figure S5N**). Pharmacological challenge with both amphetamine and PCP resulted in decreased PPI in treated mice compared to saline injected mice across all prepulse intensities. However, whereas *Brd1*$^{+/-}$ and WT mice did not differ on PPI upon amphetamine challenge (**Figure S5O**), a high dose of PCP (5 mg/kg) caused significantly decreased PPI in *Brd1*$^{+/-}$ mice compared to WT mice at 15 db intensity (**Figure 2H**, $p<0.05$). See **Figure S5P-R** and **Supplemental Results** for data on the acoustic startle responsivity (ASR) in *Brd1*$^{+/-}$ mice.

Drug responsivity, striatal neurochemistry, and transcriptome profiling

Novelty- and drug-induced hyperactivity are established rodent models of positive symptomatology in schizophrenia enabling detection of underlying neurotransmitter changes (33). Baseline locomotor activity appeared similar in *Brd1*$^{+/-}$ and WT mice with both groups showing gradual habituation to the test environment (**Figure 3A, C and Figure S6**).

Treatment with PCP, amphetamine, and cocaine all increased the activity of mice (**Figure 3A, C and Figure S6**). While no significant difference in induced activity was found between *Brd1*$^{+/-}$ and WT mice at a lower dose of PCP (2.5 mg/kg), a high dose (5 mg/kg) resulted in significantly increased horizontal locomotor activity in *Brd1*$^{+/-}$ mice (**Figure 3A**, effect of genotype, $F_{1,22}=5.9$, $p<0.05$ and **Figure 3B**, $p<0.01$) whereas rearing activity remained similar (data not shown). Cocaine caused a left-shift in the activity profile at the highest dose (30 mg/kg) with *Brd1*$^{+/-}$ mice reaching peak activity earlier than WT mice (**Figure 3C**, genotype x time interaction effect, $F_{23,506}=2.043$, $p<0.01$) but did not result in increased horizontal activity in *Brd1*$^{+/-}$ mice (Figure 3D).

Additionally, *Brd1*$^{+/-}$ mice responded to even a low dose of cocaine (10 mg/kg) with a significant increase in rearing activity compared to WT mice (**Figure 3E**, $p<0.05$). Treatment with amphetamine did not result in any significant differences in activity between genotypes (**Figure S6**).

The observed psychotomimetic drug sensitivity in *Brd1*$^{+/-}$ mice points to changes in several striatal neurotransmitter systems - including striatal monoamine neurotransmission, which has traditionally been seen as a key pathological process in schizophrenia (34; 35). Accordingly, we measured total striatal dopamine (DA), 3,4-dihydroxyphenylacetic acid (DOPAC), homovanillic acid (HVA), and serotonin (5-HT) levels in tissue extracts and found a significant increase in both DA and 5-HT in *Brd1*$^{+/-}$ mice compared to WT mice (**Figure 3F-G**, $p<0.05$), whereas DOPAC and HVA levels were similar (**Figure 3F**). For more data on neurochemistry in *Brd1*$^{+/-}$ mice see **Figure S7** and **Supplemental Results**.

Due to the putative role of BRD1 as a transcriptional regulator during neurodevelopment and in the adult brain, we performed genome-wide transcriptome profiling of tissue micro-punches obtained from the dorsal striatum using RNAseq to assess transcriptomic differences between *Brd1*$^{+/-}$ and WT mice. This analysis revealed 1378 nominally significant differentially expressed genes (DEGs; 397 downregulated and 981 upregulated) of which 269 (37 downregulated and 232 upregulated) were significant after Benjamini-Hochberg false discovery rate (FDR) correction at 5% (**Table S3**). Ingenuity Pathway analysis (IPA) of the nominally significant DEGs revealed significant enrichment ($p<0.05$) of pathways including G-protein coupled receptor signaling, cAMP mediated signaling, Protein kinase A (PKA) signaling, Dopamine-DARPP-32 feedback in cAMP signaling, and CREB (cAMP Responsive Element Binding Protein) signaling as well as DA receptor, 5-HT receptor, glutamate receptor, and GABA receptor signaling among others (**Table S4**). Remarkably, the entire annotated network of genes involved with 'Behavior, Hereditary disorder and

Neurological disease' were represented among the DEGs (p<3E-30), including the typical antipsychotic drug target gene and schizophrenia risk gene (2), *Drd2*, encoding the DA receptor D2 (**Figure S8**). Using high throughput qPCR, we validated differential expression of 34 out of 50 randomly selected FDR significant DEGs in RNA samples extracted from tissue micro-punches from independent biological replicates, indicating approximately 70% positive predictive value in the performed analysis (**Table S3**). In support of altered striatal DA transmission, we specifically validated both decreased *Drd2* mRNA (**Table S3**) and Drd2 protein levels in *Brd1*$^{+/-}$ mice (**Figure 3H**, p<0.05).

Neuronal excitability and synaptic inhibition

As *Brd1*$^{+/-}$ mice showed increased sensitivity to PCP in tests of cognition and PPI, we speculated that imbalanced excitation-inhibition might be a general cerebral feature in *Brd1*$^{+/-}$ mice. To coarsely examine if cortical GABAergic inhibitory tone is affected in *Brd1*$^{+/-}$ mice, we administered mice with various doses of the GABA-A receptor antagonist, PTZ, and observed for seizure activity. *Brd1*$^{+/-}$ mice displayed increased propensity for myoclonic jerks at 70 mg/kg (**Figure 4A**, p<0.05), despite experiencing significantly more recurrent clonic seizures within the session (**Figure 4B**, p<0.05). They further showed decreased latency to clonic seizure onset compared to WT mice across all doses (**Figure 4C**, p<0.05), whereas the fraction that experienced clonic-tonic seizures was the same (**Figure S9**).

In order to assess inhibition at the synaptic level, we performed whole-cell patch-clamp recordings of inhibitory postsynaptic currents from pyramidal neurons in layers 2/3 of the aCC in acute coronal brain slices. In the presence of kynurenic acid, an inhibitor of ionotropic glutamate receptors, we found a ~40% decrease in the frequency of spontaneous inhibitory postsynaptic currents (sIPSCs) in *Brd1*$^{+/-}$ compared to WT mice (**Figure 4D-E and H**, **Table S5**, p<0.05). We repeated the experiments in the presence of the Na^+ channel blocker, tetrodotoxin (TTX), to isolate miniature

IPSCs (mIPSCs) and found a ~38% decrease in their frequency (**Figure 4F-G and I**; **Table S5**, $p<0.01$). There was no significant difference in sIPCSs or mIPSCs mean amplitudes (**Figure 4J-K**; **Table S5**) or time parameters between *Brd1*$^{+/-}$ and WT mice. Similar findings were made in pyramidal neurons of the somatosensory cortex (**Table S5**), supporting a widespread cerebral GABAergic dysfunction in *Brd1*$^{+/-}$ mice.

Cortical gene expression profiling and Pvalb immunohistochemistry

Addressing the molecular mechanisms underlying altered cortical inhibition in *Brd1*$^{+/-}$ mice, we performed transcriptional profiling on RNA extracted from aCC tissue micro-punches by RNAseq. The analysis revealed 919 nominally significant DEGs (451 downregulated and 468 upregulated) of which 118 (61 down-regulated and 57 up-regulated) were significant after FDR correction at 5% (**Table S6**). Although less convincing than for DEGs detected in striatum, by IPA pathway analyses nominally significant DEGs were found to cluster in several canonical pathways ($p<0.05$)(**Table S7)**, including TGF-β signaling, Dopamine-DARPP32 feedback in cAMP signaling, and in accordance with the observed increase in PCP sensitivity, Glutamate receptor signaling. In the latter, genes encoding ion channels (*Grik3*, *Grik5*, *Grid2, Grin2b,* and *Grin2d),* G-protein coupled receptors (*Grm1* and *Grm2*), post-synaptic density protein (*Dlg4*), and vesicular glutamate transporter (*Slc17a7*) were upregulated whereas *Homer1,* encoding a post-synaptic density scaffolding protein, was down-regulated in *Brd1*$^{+/-}$ mice (**Figure S10**). In relation to altered inhibitory signaling in *Brd1*$^{+/-}$ mice, the marker for fast-spiking interneurons, *Pvalb*, was significantly downregulated by ~25% (**Table S6)**. To assess whether this reduction in *Pvalb* mRNA was associated with a reduction in the number of Pvalb immunoreactive cells, we further estimated the number of this sub-class of interneurons in the aCC by immunohistochemistry coupled with stereological counting and found an overall ~28% reduction (**Figure 4L,** $p<0.05$**).**

Identification of DEG upstream regulators

Overall, nominally significant DEGs identified in aCC overlapped significantly with those identified in striatum (**Table S6**, Chi^2, $p<0.001$).

Supportive of a common regulatory mechanism underlying the transcriptomic changes seen in different brain regions, IPA upstream regulator analyses of the nominally significant DEGs identified in striatum and aCC, respectively, both pointed to CREB1, BDNF, and HTT as the most likely upstream regulators of the DEGs (**Table S8,** $p<1E-5$ for all). Strikingly, this similarity in upstream regulators of the DEGs occurred despite a limited overlap in the specific DEGs identifying these regulators in the two brain regions investigated (**Table S8**). Since phosphorylation and thus activation of CREB is the downstream effect of GPCR-cAMP-DARPP-32 signaling (36) and DEGs from both striatum and aCC cluster in this pathway, we investigated Creb phosophorylation in whole-brain protein extracts. We found that Creb was hyper-phosphorylated in *Brd1*$^{+/-}$ mice compared to WT mice (**Figure 5A**, $p<0.05$) and further, that its transcriptional target, c-Fos, was significantly more abundant (**Figure 5A**, $p<0.05$).

Schizophrenia risk enrichment in DEG sets

Using summary statistics from the largest to date schizophrenia GWAS (2), we assessed risk enrichment by MAGMA (20) analysis of DEGs from both aCC and striatum - and the two regions combined. Interestingly, we found that DEGs from each brain region, separately, was enriched with schizophrenia risk (**Figure S11**, $p<0.05$) and more significantly when the two regions were assessed collectively (**Figure S11**, $p<0.01$). In a secondary exploratory analysis, we assessed whether DEGs were enriched for common variant risk in other disorders/traits. Besides from DEGs in aCC, which showed enrichment for bipolar disorder (**Figure S11**, $p<0.05$), no risk enrichment was seen for other brain and non-brain disorders/traits (**Figure S11**). In line with the identified schizophrenia risk enrichment, we found that a significant higher proportion of striatum and aCC DEGs localize to

genome-wide significant schizophrenia risk loci than expected by chance (**Table S9**, $p<0.01$), including loci containing e.g. the calcium channel subunits genes, *Cacna1c* and *Cacnb2*, the cholinergic muscarinic receptor 4 gene, C*hrm4*, *Drd2*, and the transcription factor 4 gene, *Tcf4*. Noteworthy in this context, the 3'UTR of *BRD1* contains a conserved target site for microRNA-137, which is also is located in a schizophrenia GWAS locus (37).

Discussion

BRD1 is located in a 150 kb haploblock comprising the four genes *ALG12*, *CRELD2*, *ZBED4*, and *BRD1*. In addition to the genetic associations and the schizophrenia risk enrichment of BRD1's chromatin interactome reported previously (12), the present study provides evidence strongly suggesting *BRD1* as the causal risk gene within the locus. We show that *BRD1* schizophrenia risk alleles correlate with reduced *BRD1* expression and we provide direct *in vitro* evidence that the rs138880 risk allele lowers transcriptional drive. Moreover, we generate mice with reduced *Brd1* expression and find that they display hypersensitivity to psychostimulants and behavioral abnormalities with translational relevance to schizophrenia symptomatology along with changes in neuro-chemistry and –transmission reminiscent of findings in schizophrenia. In accordance with a central role for BRD1 as a transcriptional regulator in the brain, we establish that decreased expression of *Brd1* in mice leads to cerebral histone H3K14 hypo-acetylation and extensive changes in expression of genes that are enriched for schizophrenia risk and cluster in functional networks associated with mental disorders. Finally, it may be noted that neurological screenings of knockout mouse models for *Creld2* and *Zbed4* have not revealed phenotypes with translational relevance to schizophrenia symptomatology (38).

Schizophrenia is a highly polygenic disorder with small effect sizes of the implicated common risk variants. The rs138880 *BRD1* promoter variant contribute to schizophrenia risk with an estimated odds ratio of around 1.1 (8), which is likely reflected in the discrete expression phenotypic effect that we observe in risk allele carriers. Hence, the *Brd1*$^{+/-}$ mouse with a ~50% reduction of *Brd1* expression does not exactly reflect the effect associated with the risk allele, but rather demonstrate the molecular and functional consequences of hampered *BRD1* expression. However, despite *BRD1* being very intolerant to loss of function mutations (39), a schizophrenia patient carrying a nonsense mutation in *BRD1* disrupting the gene in the first exon has recently been

detected in a large schizophrenia exome-sequencing study (40), thus more directly parallelizing the *Brd1*$^{+/-}$ mouse. Furthermore, in terms of global cerebral H3 hypo-acetylation – a trait that has been shown in young subjects with schizophrenia and which correlate with expression levels of genes implicated with psychiatric disorders (41) - this effect in the mice is within a clinically relevant range. Finally, by influencing histone modification and thereby the chromatin state around genes in its comprehensive schizophrenia risk enriched chromatin interactome, the presented modulation of *Brd1* expression may be conceived as a way to model the highly polygenic nature of schizophrenia.

Social behavior, cognition, PCP sensitivity, and cortical neurotransmission

Negative symptoms reflect a range of deficits in normal emotional responses in individuals with schizophrenia. In mice, assessment of this domain is largely confined to tests for social interaction and general sociability. Our findings that *Brd1*$^{+/-}$ mice showed markedly different social interaction profiles and impaired ability to recall social identifiers may collectively have translational relevance to the social withdrawal (42) and social recognition deficits (43) observed in schizophrenia.

Also with translational relevance to schizophrenia symptomatology (44; 45), we observed clear deficits in associative learning in *Brd1*$^{+/-}$ mice and an accelerated time-dependent loss of acquired contextual memories. Indicative of a reduced capacity in the glutamatergic transmission to support pre-attentive processing and cognition, *Brd1*$^{+/-}$ mice displayed increased sensitivity to the disruptive effect of PCP on PPI and working memory performance.

We speculate that primarily altered neurotransmission may underlie the cognitive deficits and increased sensitivity to PCP in *Brd1*$^{+/-}$ mice. In agreement, *Brd1*$^{+/-}$ mice displayed elevated seizure propensity in response to PTZ, suggestive of increased excitability of critical neurocircuitry. Furthermore, evaluation of sIPSCs and mIPSCs by patch-clamp recordings from pyramidal neurons demonstrated a clear deficit in inhibitory GABAergic synaptic neurotransmission in the aCC, which

co-incited with a significant up-regulation of genes encoding glutamatergic receptors and a specific decrease in Pvalb immunoreactive fast-spiking interneurons in this tissue.

In support of altered cortical excitability (46), transcriptome data revealed differential expression of DA receptor D1 (*Drd1a*) and disturbed DA-DARPP-32 signaling which has been linked to cognitive performance (47), sensorimotor gating (36), and general prefrontal dysfunction in schizophrenia cases (48).

Psychotomimetic drug response and striatal neuro-chemistry and -signaling

Positive symptoms arise from altered striatal dopaminergic transmission (49), and psychotic symptoms are inducible even in healthy individuals by administration of drugs that increase striatal DA activity. Similarly, sensitivity to psychostimulants is used to mimic psychosis-like behavior in mice using locomotor activity as a read-out for increased striatal DA activity.
Decreased levels of *Brd1* sensitize mice to both the effect of PCP and cocaine in a manner reminiscent of the enhanced sensitivity that individuals with schizophrenia display to psychostimulant drugs (50) - but in contrast to what is observed in patients, this sensitization was not evident following amphetamine challenge. The locomotor stimulatory effect of PCP is exerted through several mechanisms aside from the direct effect of blocking NMDA receptors, including actions at DA- and 5-HT receptors (51; 52), and it has been shown to rely on DARPP-32 facilitated striatonigral signaling (53). Amphetamine and cocaine both inhibit the reuptake of monoamines and, similar to what has been observed in individuals with schizophrenia (54), both striatal DA and 5-HT levels were significantly elevated in *Brd1*$^{+/-}$ mice. However, whereas cocaine relies on DA release to exert its effect (55–57), amphetamine mediates its psychomotor-stimulatory effect in a firing independent way (58). Striatal DA release is determined by DA release probability (59; 60) which is profoundly controlled by cholinergic interneurons in striatum (61). Noteworthy, we found that two of the main cholinergic receptors, *Chrna2* and *Chrm4*, responsible for the dynamic control

of DA release probability are differentially regulated in striatal tissue of *Brd1*$^{+/-}$ mice (61) – thus offering a possible explanation for the selective drug sensitivity displayed by *Brd1*$^{+/-}$ mice.

In concordance with altered DA and 5-HT transmission, transcriptome profiling of striatal tissue revealed reduced expression of both DA receptor D1 (*Drd1a*), D2 (*Drd2*) and differential expression of several 5-HT receptors. The effect of reduced *Brd1* expression on the striatal transcriptome is, however, widespread and suggests dysregulation of multiple signaling pathways that ultimately appears to converge in the DARPP-32 signaling pathway of striatal medium spiny neurons (MSNs) (**Figure 5B** and **Figure S12**). Our finding that Creb was globally hyper-phosphorylated and that its transcriptional target, c-Fos globally more abundant in the *Brd1*$^{+/-}$ mice strongly supports that DARPP-32 signaling is affected.

Enrichment of schizophrenia risk

Emphasizing the importance of BRD1 as a cardinal transcriptional regulator, we demonstrate widespread expression alterations in the brains of *Brd1*$^{+/-}$ mice. This includes altered expression of transcriptional regulators and immediate early genes (IEGs) like *Homer*, *Bdnf*, *c-fos*, *c-jun,* and *Shank* which have previously been linked to the etiopathology of mental disorders (62–64). We further find that the identified DEGs are enriched for schizophrenia risk and that they cluster within known GWAS schizophrenia risk loci. In accordance with this, DEGs group in pathways that largely overlap with the recently published pathway analysis of GWAS data (65). Thus, the identified pathways are not only centered on calcium signaling and synaptic and postsynapse-related processes but also comprise diverse immune, hormonal, and signal transduction pathways – including CREB (65).

During recent years, the hunt for schizophrenia susceptibility genes through large scale GWASs has revealed SNPs statistically associated with the disorder but yet provided little information on their functional contribution to the pathogenesis. In general, GWAS-identified markers seem to play a major role in the regulation of gene expression rather than the alteration of protein sequence (66; 67). We demonstrate that a risk allele in the *BRD1* promoter is associated with reduced *BRD1* expression, which in mice result in widespread transcriptomic changes that to a high extent affect schizophrenia risk loci and cluster in networks and pathways associated with mental disorders. Reduced Brd1 expression causes epigenetic alterations involving cerebral histone H3 hypoacetylation which, in line with the dominating hypotheses of schizophrenia, ultimately results in developmental loss of Pvalb immunoreactive interneurons, imbalanced excitatory/inhibitory neurotransmission, region-specific changes in monoamine neurochemistry and behavioral abnormalities translating to major categories of schizophrenia symptomatology (**Table 1**). Underlining the pharmaceutical relevance of the presented neuro-molecular and -chemical consequences of Brd1 deficiency, epigenetic therapy has been shown to be effective in treating aspects of mental illness (68; 69) and histone deacetylase inhibitor drugs are currently undergoing clinical trials for the treatment of cognitive deficits in schizophrenia (70).

Acknowledgements

We acknowledge Anne Hedemand and Stine Lund for extensive genotyping of mice, Nina Guldhammer for processing HPLC samples, Jakob Grove for statistical assistance and Helene M. Andersen and Maj-Britt Lundorf for assisting in IHC experiments.

The study was supported by grants from The Danish Council for Independent Research | Medical Sciences, The Lundbeck Foundation, The Faculty of Health Sciences, Aarhus University, and The Novo Nordisk Foundation. Centre for Stochastic Geometry and Advanced Bioimaging was supported by Villum Foundation.

We thank the International Genomics of Alzheimer's Project (IGAP) for providing summary results data for these analyses. The investigators within IGAP contributed to the design and implementation of IGAP and/or provided data but did not participate in analysis or writing of this report. IGAP was made possible by the generous participation of the control subjects, the patients, and their families. The i–Select chips were funded by the French National Foundation on Alzheimer's disease and related disorders. EADI was supported by the LABEX (laboratory of excellence program investment for the future) DISTALZ grant, Inserm, Institut Pasteur de Lille, Université de Lille 2 and the Lille University Hospital. GERAD was supported by the Medical Research Council (Grant n° 503480), Alzheimer's Research UK (Grant n° 503176), the Wellcome Trust (Grant n° 082604/2/07/Z) and German Federal Ministry of Education and Research (BMBF): Competence Network Dementia (CND) grant n° 01GI0102, 01GI0711, 01GI0420. CHARGE was partly supported by the NIH/NIA grant R01 AG033193 and the NIA AG081220 and AGES contract N01–AG–12100, the NHLBI grant R01 HL105756, the Icelandic Heart Association, and the Erasmus Medical Center and Erasmus University. ADGC was supported by the NIH/NIA

grants: U01 AG032984, U24 AG021886, U01 AG016976, and the Alzheimer's Association grant ADGC–10–196728.

Financial Disclosures

OM and ADB are co-inventors on a patent application submitted by Aarhus University entitled "Method for diagnosis and treatment of a mental disease" (EP20060742417) that includes claims relating to *BRD1* among other genes. OM, ADB, JHC, APR, MN, and PQ are co-inventors on a patent application submitted by Capnova A/S entitled "Genetically modified non-human mammal and uses thereof" (PCT/EP2013/069524) that includes the *Brd1*$^{+/-}$ mouse.

Besides being employed by H. Lundbeck A/S, KF, AM, and MD declares no biomedical financial interests or potential conflicts of interest.

IV, VP, EMF, TF, JP, MD, MEH, BL, KJ, and JRN report no biomedical financial interests or potential conflicts of interest.

Contributions

PQ, JHC, MD, and ADB designed and directed the experiments. PQ, JHC, and ADB wrote the manuscript. PQ performed the majority of experiments. ADB, JHC, and MN designed the genetically modified *Brd1*$^{+/-}$ mouse. JHC managed the breeding of the mice. AM designed HPLC experiments. IV and KJ designed and performed electrophysiological experiments. EMF and JHC analyzed mouse embryos. VP measured *Brd1* RNA and protein levels in *Brd1*$^{+/-}$ mice. PQ and TF conducted further protein analyses. JHC, MDY, and BL performed dual luciferase reporter assay. KF designed ASR and PPI setup. APR, PQ, ADB, and JHC designed, conducted, and analyzed RNAseq experiments. JRN and PQ designed and conducted stereological studies. MEH and JP performed enrichment analyses. PQ, APR, and JP performed the statistical analyses. ADB and OM

conceived the basic idea and initiated the study. MD, OM, JHC, and ADB designed and directed the study. All authors have read and approved the final manuscript.

REFERENCES

1. Ripke S, O'Dushlaine C, Chambert K, Moran JL, Kähler AK, Akterin S, *et al.* (2013): Genome-wide association analysis identifies 13 new risk loci for schizophrenia. *Nat Genet*. 45: 1150–9.

2. Ripke S, Neale BM, Corvin A, Walters JTR, Farh K-H, Holmans PA, *et al.* (2014): Biological insights from 108 schizophrenia-associated genetic loci. *Nature*. 511: 421–427.

3. Coon, H., Jensen, S., Holik, J., Hoff, M., Myles-Worsley, M., Reimherr, F., Wender, P., Waldo, M., Freedman, R., Leppert, M. and Byerley W (1994): Genomic scan for genes predisposing to schizophrenia. *Am J Med Genet*. 54: 59–71.

4. Pulver AE, Karayiorgou M, Wolyniec PS, Lasseter VK, Kasch L, Nestadt G, *et al.* (1994): Sequential strategy to identify a susceptibility gene for schizophrenia: report of potential linkage on chromosome 22q12-q13.1: Part 1. *Am J Med Genet*. 54: 36.

5. Jorgensen TH, Borglum AD, Mors O, Wang AG, Pinaud M, Flint TJ, *et al.* (2002): Search for Common Haplotypes on Chromosome 22q in Patients With Schizophrenia or Bipolar Disorder From the Faroe Islands. *Am J Med Genet*. 114: 245–252.

6. Severinsen JE, Bjarkam CR, Kiaer-Larsen S, Olsen IM, Nielsen MM, Blechingberg J, *et al.* (2006): Evidence implicating BRD1 with brain development and susceptibility to both schizophrenia and bipolar affective disorder. *Mol Psychiatry*. 11: 1126–38.

7. Nyegaard M, Severinsen JE, Als TD, Hedemand A, Straarup S, Nordentoft M, *et al.* (2010): Support of association between BRD1 and both schizophrenia and bipolar affective disorder. *"American J Med Genet Part B, Neuropsychiatr Genet Off Publ Int Soc Psychiatr Genet*. 153B: 582–91.

8. Aberg K a, Liu Y, Bukszár J, McClay JL, Khachane AN, Andreassen O a, *et al.* (2013): A comprehensive family-based replication study of schizophrenia genes. *JAMA Psychiatry*. 70: 1–9.

9. Andreassen OA, Thompson WK, Dale AM (2014): Boosting the power of schizophrenia genetics by leveraging new statistical tools. *Schizophr Bull*. 40: 13–17.

10. Doyon Y, Cayrou C, Ullah M, Landry A-J, Côté V, Selleck W, *et al.* (2006): ING tumor suppressor proteins are critical regulators of chromatin acetylation required for genome expression and perpetuation. *Mol Cell*. 21: 51–64.

11. Mishima Y, Miyagi S, Saraya A, Negishi M, Endoh M, Endo TA, *et al.* (2011): The Hbo1-Brd1/Brpf2 complex is responsible for global acetylation of H3K14 and required for fetal liver erythropoiesis. *Blood*. 118: 2443–53.

12. Fryland T, Christensen JH, Pallesen J, Mattheisen M, Palmfeldt J, Bak M, *et al.* (2016): Identification of the BRD1 interaction network and its impact on mental disorder risk. *Genome Med*. 8: 53.

13. Colantuoni C, Lipska BK, Ye T, Hyde TM, Tao R, Leek JT, *et al.* (2011): Temporal dynamics

and genetic control of transcription in the human prefrontal cortex. *Nature*. 478: 519–523.

14. Bjarkam CR, Corydon TJ, Olsen IML, Pallesen J, Nyegaard M, Fryland T, *et al.* (2009): Further immunohistochemical characterization of BRD1 a new susceptibility gene for schizophrenia and bipolar affective disorder. *Brain Struct Funct*. 214: 37–47.

15. Fryland T, Elfving B, Christensen JH, Mors O, Wegener G, Børglum AD (2012): Electroconvulsive seizures regulates the Brd1 gene in the frontal cortex and hippocampus of the adult rat. *Neurosci Lett*. 516: 110–113.

16. Christensen JH, Elfving B, Müller HK, Fryland T, Nyegaard M, Corydon TJ, *et al.* (2012): The Schizophrenia and Bipolar Disorder associated BRD1 gene is regulated upon chronic restraint stress. *Eur Neuropsychopharmacol*. 22: 651–6.

17. Lee S, Ripke S, Neale BM, Faraone SV, Purcell SM, Perlis RH, Mowry BJ, Thapar A, Goddard ME, Witte JS, Absher D, Agartz I, Akil H, Amin F, Andreassen OA, Anjorin A, Anney R, Anttila V, Arking DE, Asherson P, Azevedo MH, Backlund L, Badner JA, Bailey AJ, WN (2013): Systematic identification of trans eQTLs as putative drivers of known disease associations. *Nat Genet*. 45: 1238–1243.

18. Paxinos G, Franklin KBJ (2001): *The mouse brain in stereotaxic coordinates*, 2nd ed. Academic press.

19. Rajkumar AP, Qvist P, Lazarus R, Lescai F, Ju J, Nyegaard M, *et al.* (2015): Experimental validation of methods for differential gene expression analysis and sample pooling in RNA-seq. *BMC Genomics*. 16: 548.

20. de Leeuw C a., Mooij JM, Heskes T, Posthuma D (2015): MAGMA: Generalized Gene-Set Analysis of GWAS Data. *PLOS Comput Biol*. 11: e1004219.

21. Stranger BE, Montgomery SB, Dimas AS, Parts L, Stegle O, Ingle CE, *et al.* (2012): Patterns of cis regulatory variation in diverse human populations. *PLoS Genet*. 8: e1002639.

22. Purcell SM, Wray NR, Stone JL, Visscher PM, O'Donovan MC, Sullivan PF, Sklar P (2009): Common polygenic variation contributes to risk of schizophrenia and bipolar disorder. *Nature*. 460: 748–52.

23. Ardlie KG, Deluca DS, Segre A V., Sullivan TJ, Young TR, Gelfand ET, *et al.* (2015): The Genotype-Tissue Expression (GTEx) pilot analysis: Multitissue gene regulation in humans. *Science (80-)*. 348: 648–660.

24. Young JW, Powell SB, Risbrough V, Marston HM, Geyer M a (2009): Using the MATRICS to guide development of a preclinical cognitive test battery for research in schizophrenia. *Pharmacol Ther*. 122: 150–202.

25. Jones C, Watson D, Fone K (2011): Animal models of schizophrenia. *Br J Pharmacol*. 164: 1162–1194.

26. O'Tuathaigh CM, Waddington JL (2015): Closing the translational gap between mutant mouse models and the clinical reality of psychotic illness. *Neurosci Biobehav Rev*. 58: 19–35.

27. Floresco SB, Geyer MA, Gold LH, Grace AA (2005): Developing predictive animal models and establishing a preclinical trials network for assessing treatment effects on cognition in schizophrenia. *Schizophr Bull*. 31: 888–94.

28. Braff D, Geyer M, Swerdlow N (2001): Human studies of prepulse inhibition of startle: normal subjects, patient groups, and pharmacological studies. *Psychopharmacology (Berl)*. 156: 234–258.

29. Leavitt VM, Molholm S, Ritter W, Shpaner M, Foxe JJ (2007): Auditory processing in schizophrenia during the middle latency period (10-50 ms): high-density electrical mapping and source analysis reveal subcortical antecedents to early cortical deficits. *J Psychiatry Neurosci*. 32: 339–53.

30. Karl T, Pabst R, von Hörsten S (2003): Behavioral phenotyping of mice in pharmacological and toxicological research. *Exp Toxicol Pathol*. 55: 69–83.

31. Gogos A, van den Buuse M, Rossell S (2009): Gender differences in prepulse inhibition (PPI) in bipolar disorder: men have reduced PPI, women have increased PPI. *Int J Neuropsychopharmacol*. 12: 1249–59.

32. Braff DL (1990): Sensorimotor Gating and Schizophrenia - Human and Animal Model Studies. *Arch Gen Psychiatry*. 47: 181.

33. van den Buuse M (2010): Modeling the positive symptoms of schizophrenia in genetically modified mice: pharmacology and methodology aspects. *Schizophr Bull*. 36: 246–70.

34. Moore H, West AR, Grace AA (1999): The regulation of forebrain dopamine transmission: relevance to the pathophysiology and psychopathology of schizophrenia. *Biol Psychiatry*. 46: 40–55.

35. Geyer, M., Moghaddam B (2002): Neuropsychopharmacology: The fifth generation of progress. In: K. L. Davis, D. Charney, J. T. Coyle, C. Nemeroff. Lippincott W and W, editor. *Hum Psychopharmacol Clin Exp*. (Vol. 17), Philadelphia, pp 433–433.

36. Svenningsson P, Tzavara ET, Carruthers R, Rachleff I, Wattler S, Nehls M, *et al.* (2003): Diverse psychotomimetics act through a common signaling pathway. *Science*. 302: 1412–5.

37. Agarwal V, Bell GW, Nam J-W, Bartel DP (2015): Predicting effective microRNA target sites in mammalian mRNAs. *Elife*. 4. doi: 10.7554/eLife.05005.

38. Skarnes WC, Rosen B, West AP, Koutsourakis M, Bushell W, Iyer V, *et al.* (2011): A conditional knockout resource for the genome-wide study of mouse gene function. *Nature*. 474: 337–342.

39. Exome Aggregation Consortium (ExAC) (n.d.): . Retrieved November 3, 2016, from http://exac.broadinstitute.org/.

40. Purcell SM, Moran JL, Fromer M, Ruderfer D, Solovieff N, Roussos P, *et al.* (2014): A polygenic burden of rare disruptive mutations in schizophrenia. *Nature*. 506: 185–90.

41. Tang B, Dean B, Thomas EA (2011): Disease- and age-related changes in histone acetylation at gene promoters in psychiatric disorders. *Transl Psychiatry*. 1.

42. Andreasen N (1982): Negative symptoms in schizophrenia: definition and reliability. *Arch Gen Psychiatry*. 39: 784–8.

43. Brunet-Gouet E, Decety J (2006): Social brain dysfunctions in schizophrenia: a review of neuroimaging studies. *Psychiatry Res*. 148: 75–92.

44. Jensen J, Willeit M, Zipursky RB, Savina I, Smith AJ, Menon M, *et al.* (2008): The formation of abnormal associations in schizophrenia: neural and behavioral evidence. *Neuropsychopharmacology*. 33: 473–9.

45. Hofer E, Doby D, Anderer P, Dantendorfer K (2001): Impaired conditional discrimination learning in schizophrenia. *Schizophr Res*. 51: 127–36.

46. Tseng KY, O'Donnell P (2004): Dopamine-Glutamate Interactions Controlling Prefrontal

Cortical Pyramidal Cell Excitability Involve Multiple Signaling Mechanisms. *J Neurosci*. 24: 5131–5139.

47. Hotte M, Thuault S, Lachaise F, Dineley KT, Hemmings HC, Nairn AC, Jay TM (2006): D1 receptor modulation of memory retrieval performance is associated with changes in pCREB and pDARPP-32 in rat prefrontal cortex. *Behav Brain Res*. 171: 127–33.

48. Albert KA, Hemmings HC, Adamo AIB, Potkin SG, Akbarian S, Sandman CA, *et al.* (2002): Evidence for decreased DARPP-32 in the prefrontal cortex of patients with schizophrenia. *Arch Gen Psychiatry*. 59: 705–12.

49. Coyle JT, Tsai G, Goff D (2003): Converging Evidence of NMDA Receptor Hypofunction in the Pathophysiology of Schizophrenia. *Ann N Y Acad Sci*. 1003: 318–327.

50. Lieberman JA, Kane JM, Alvir J (1987): Provocative tests with psychostimulant drugs in schizophrenia. *Psychopharmacology (Berl)*. 91: 415–33.

51. Kapur S, Seeman P (2002): NMDA receptor antagonists ketamine and PCP have direct effects on the dopamine D2 and serotonin 5-HT2receptors—implications for models of schizophrenia. *Mol Psychiatry*. 7: 837–844.

52. Johnson KM, Jones SM (1990): Neuropharmacology of Phencyclidine: Basic Mechanisms and Therapeutic Potential. *Annu Rev Pharmacol Toxicol*. 30: 707–750.

53. Bonito-Oliva A, DuPont C, Madjid N, Ögren SO, Fisone G (2015): Involvement of the Striatal Medium Spiny Neurons of the Direct Pathway in the Motor Stimulant Effects of Phencyclidine. *Int J Neuropsychopharmacol*. pyv134.

54. Laruelle M (1996): Single photon emission computerized tomography imaging of amphetamine-induced dopamine release in drug-free schizophrenic subjects. *Proc Natl Acad Sci U S A*. 93: 9235–9240.

55. White FJ (1990): Electrophysiological basis of the reinforcing effects of cocaine. *Behav Pharmacol*. 1: 303–315.

56. Iversen L (2009): *Dopamine Handbook*. (L. Iversen, S. Iversen, S. Dunnett, & A. Bjorklund, editors). Oxford University Press. doi: 10.1093/acprof:oso/9780195373035.001.0001.

57. Stahl SM (2013): *Essential psychopharmacology: Neuroscientific basis and practical applications*, 4th ed. Cambridge University Press.

58. Freyberg Z, Sonders MS, Aguilar JI, Hiranita T, Karam CS, Flores J, *et al.* (2016): Mechanisms of amphetamine action illuminated through optical monitoring of dopamine synaptic vesicles in Drosophila brain. *Nat Commun*. 7: 10652.

59. Chergui K, Suaud-Chagny MF, Gonon F (1994): Nonlinear relationship between impulse flow, dopamine release and dopamine elimination in the rat brain in vivo. *Neuroscience*. 62: 641–5.

60. Montague PR, McClure SM, Baldwin PR, Phillips PEM, Budygin EA, Stuber GD, *et al.* (2004): Dynamic gain control of dopamine delivery in freely moving animals. *J Neurosci*. 24: 1754–9.

61. Threlfell S, Cragg SJ (2011): Dopamine Signaling in Dorsal Versus Ventral Striatum: The Dynamic Role of Cholinergic Interneurons. *Front Syst Neurosci*. 5: 11.

62. Kyosseva S V (2004): Differential expression of mitogen-activated protein kinases and immediate early genes fos and jun in thalamus in schizophrenia. *Prog Neuropsychopharmacol Biol Psychiatry*. 28: 997–1006.

63. Todorova VK, Elbein AD, Kyosseva S V (2003): Increased expression of c-Jun transcription

factor in cerebellar vermis of patients with schizophrenia. *Neuropsychopharmacology*. 28: 1506–14.

64. Reul JMHM (2014): Making memories of stressful events: a journey along epigenetic, gene transcription, and signaling pathways. *Front psychiatry*. 5: 5.

65. Consortium TN and PAS of the PG (2015): Psychiatric genome-wide association study analyses implicate neuronal, immune and histone pathways. *Nat Neurosci*. 18: 199–209.

66. Maurano MT, Humbert R, Rynes E, Thurman RE, Haugen E, Wang H, *et al.* (2012): Systematic localization of common disease-associated variation in regulatory DNA. *Science*. 337: 1190–5.

67. Hindorff LA, Sethupathy P, Junkins HA, Ramos EM, Mehta JP, Collins FS, Manolio TA (2009): Potential etiologic and functional implications of genome-wide association loci for human diseases and traits. *Proc Natl Acad Sci*. 106: 9362–9367.

68. Cipriani A, Reid K, Young AH, Macritchie K, Geddes J (2013): Valproic acid, valproate and divalproex in the maintenance treatment of bipolar disorder. In: Geddes J, editor. *Cochrane Database Syst Rev*. Chichester, UK: John Wiley & Sons, Ltd. doi: 10.1002/14651858.CD003196.pub2.

69. Schwarz C, Volz A, Li C, Leucht S (2008): Valproate for schizophrenia. In: Schwarz C, editor. *Cochrane Database Syst Rev*. Chichester, UK: John Wiley & Sons, Ltd. doi: 10.1002/14651858.CD004028.pub3.

70. Kline N (2016): Sodium Butyrate For Improving Cognitive Function In Schizophrenia NLM Identifier: NCT02654405. *Clin [Internet], Bethesda Natl Libr Med*. . Retrieved from https://clinicaltrials.gov/ct2/show/NCT02654405.

71. Hemmings HC, Greengard P, Tung HY, Cohen P (n.d.): DARPP-32, a dopamine-regulated neuronal phosphoprotein, is a potent inhibitor of protein phosphatase-1. *Nature*. 310: 503–5.

72. Esteban JA, Shi S-H, Wilson C, Nuriya M, Huganir RL, Malinow R (2003): PKA phosphorylation of AMPA receptor subunits controls synaptic trafficking underlying plasticity. *Nat Neurosci*. 6: 136–143.

73. Greengard P, Allen PB, Nairn AC (1999): Beyond the Dopamine Receptor. *Neuron*. 23: 435–447.

74. Berke JD, Hyman SE (2000): Addiction, dopamine, and the molecular mechanisms of memory. *Neuron*. 25: 515–32.

LEGENDS

Figure 1

***BRD1* schizophrenia risk variants associate with reduced *BRD1* expression. (A)** Plotted is the normalized expression in blood of the ILMN_1730019 probe, which is located in the 3'UTR of the *BRD1* gene, for rs138880 non-risk (AA) and risk (AC, no homozygous carriers among genotyped subjects) allele carriers. **(B)** Similarly, in cortical tissue the normalized expression of the *BRD1* probe, hHC012627, was plotted for non-risk (GG) and risk (GA/AA) allele carriers of rs7410537 which is in strong LD with rs138880. (See **Figure S1**). *t* test was applied to compare *BRD1* expression between groups. **(C)** Dual luciferase reporter assay of *BRD1* promoter fragments containing rs138880 SNP variants (A or C allele) with schematic representation of the genomic localization (chr22:50,217,500-50,219,500; GRCh37/hg19) of *BRD1* illustrating the 5'UTR (narrow line) and the 5' part of exon 1 (broad line). Random effects meta-analysis of four independent luciferase assays (Experiment 1-4, presented in **Figure S2B**) is presented. For experiment 1, the number of replicate transfections are *n*=6 and for experiments 2-4 the number are *n*=15-16 for the A and C allele. The standardized mean difference (SMD) and 95% CI of experiment 1-4 and the total random effects are plotted. SMD=2.82, [95% CI, 1.42 to 4.21]. **(D)** Schematic representation of the WT allele of the mouse *Brd1* locus, the targeting construct used for homologous recombination in C57BL/6NTac embryonic stem cells (vector backbone omitted for clarity), the resulting targeted allele and the mutant allele derived by *in vivo* CRE-mediated deletion of exon 3-5 using a ubiquitously active general CRE deleter. **(E)** Quantitative RT-PCR analysis of *Brd1* transcripts derived from whole brain tissue from WT and $Brd1^{+/-}$ mice (*n*=6 for each genotype). Measurements of two different exon border spanning amplicons are shown (exon 3-4 is contained within the deleted region, whereas the amplicon spanning exon 11-12 is located outside this region in the 3' end of the *Brd1* transcript). *Brd1* expression in $Brd1^{+/-}$ mice was 34% (*t* test,

p<0.001) and 58% (t test, p<0.001) lower than in WT mice for respectively, the exon 3-4 and exon 11-12 amplicons. **(F)** Western blotting analysis of protein extracts derived from whole brain tissue from WT and *Brd1*$^{+/-}$ mice. Top membrane was incubated with the anti-BRD1-L (AB67) antibody (detecting a band of an apparent molecular weight of 150 kDa; predicted molecular weight of BRD1-L is 133 kDa), lower membrane half was incubated with an anti-Beta actin antibody (detecting a band of an apparent molecular weight of 42 kDa, comparable to the predicted molecular weight). Two positive control samples, derived from HEK cell lines stably expressing the V5-tagged human BRD1-L or BRD1-S isoforms, respectively, as well as a negative control, were analyzed simultaneously and incubated with an anti-V5 antibody. A band migrating similarly to the human BRD1-L control was detected in all samples and annotated as the mouse BRD1-L. Densitometric analysis of protein amounts is presented. Samples were derived from WT (n=10) and *Brd1*$^{+/-}$ (n=10) mice (1:1 male to female ratio in both groups). Protein amounts in individual samples were normalized to the amounts of Beta-actin and plotted as relative means (+ SEM) to the average protein amount of the WT group. The average BRD-L protein amount was decreased by 48% in *Brd1*$^{+/-}$ mice compared to their WT littermates (t test, p=0.079). A similar result was obtained in an independent Western blotting analysis using the same antibody but including densitometric analysis of bands derived from samples of pooled whole brain extracts (**Figure S3F**) **(G)** Level of acetylation at H3K14 relative to the amount of H4 in histone extractions from whole brain (WT and *Brd1*$^{+/-}$ male mice; n=3 for each genotype). Analysis was made by Western blotting using the indicated antibodies. Densitometric analysis of relative acetylated H3K14 protein amounts, normalized to the amounts of H4, revealed a reduction by ~19% in brains from *Brd1*$^{+/-}$ mice compared to WT mice. Comparisons between groups were performed using two-sample Student t tests. *p<0.05, **p<0.01. Data shown are mean and SEM for each group unless specifically stated otherwise.

Figure 2

***Brd1*$^{+/-}$ mice display selective deficits in social behavior, impaired performance in tests addressing social cognition, learning and memory, and affected pre-attentive processing. (A)** Social interaction between same genotype mice (*Brd1*$^{+/-}$ n=10, WT n=10). *Brd1*$^{+/-}$ mice spend less time engaged in social support than WT mice (t test, p<0.05) and display more aggressive incidences (zero-inflated poisson regression, IRR=12.67, p<0.05). **(B)** *Brd1*$^{+/-}$ mice hesitated for longer before engaging in social interaction with partner mice (t test, p<0.01). Bars represent latency to first contact between mice. **(C)** Three chamber test for sociability (*Brd1*$^{+/-}$ n=12, WT n=11). Preference score for time spend investigating a non-social (toy mouse) versus a social stimulus (stranger 1) in a 10 min. session. *Brd1*$^{+/-}$ mice investigated toy mouse (non-social stimulus) and a weight-matched unfamiliar mouse (social stimulus) without preference. This is in contrast to WT mice, which displayed a clear preference for the social stimulus (t test, p<0.001). **(D)** Three chamber test for social novelty (*Brd1*$^{+/-}$ n=12, WT n=11). Preference score for time spend investigating a familiar mouse (stranger 1) versus an unfamiliar mouse (stranger 2). *Brd1*$^{+/-}$ and WT mice both preferred to investigate a novel social stimulus rather than the previously encountered social stimulus (t test, p>0.05). **(E)** Three chamber test for remote social memory carried out one week after former two tests (*Brd1*$^{+/-}$ n=10, WT n=10). Preference score for time spend with a familiar mouse (stranger 2) encountered in the 10 min. session the previous week versus a completely new mouse (stranger 3). *Brd1*$^{+/-}$ mice lacked the preference for novelty displayed be WT mice, indicating that the memory of stranger 2 consolidated the previous week was impaired (t test, p<0.05). **(F)** Acquisition of conditioned learning in *Brd1*$^{+/-}$ mice and WT mice (*Brd1*$^{+/-}$ n=12, WT n=12). Freezing behavior was monitored during a 240 sec. training session that included 4 exposures to foot shock. *Brd1*$^{+/-}$ mice spend less time freezing than WT mice, thus demonstrating compromised contextual learning (Two-way RMANOVA, effect of genotype, $F_{1,20}$=8142, p<0.01)

with post hoc comparisons showing significantly decreased freezing behavior at exposure 2 (p<0.05), 3 (p<0.01) and 4 (p<0.05) and post-acquisition (p<0.05). **(G)** Context dependent memory retrieval was measured as freezing behavior in the test box an hour after acquisition and again 3 and 7 days after acquisition (*Brd1*$^{+/-}$ n=12, WT n=12). *Brd1*$^{+/-}$ mice displayed similar freezing behavior as WT mice an hour after acquisition, demonstrating that they had learned the relation between context and foot shock (t test, p<0.05). When placed in the same context 3 days later, *Brd1*$^{+/-}$ mice showed less freezing behavior than WT mice, indicating that they were less capable of recalling the conditioned contextual memory (t test, p<0.01). This was even more prominent when measured 7 days after acquisition (t test, p<0.001). **(H)** Mice were tested for PPI in 3 sessions spanning 4 days and including habituation to the test paradigm on day 1 (not shown), baseline testing on day 3 (not shown), and psychotropic challenge on day 4. Mice were administered a single dose of PCP (5 mg/kg shown) and tested across 3 intensities (5, 10, and 15db above background level). *Brd1*$^{+/-}$ mice were significantly more sensitive to the PPI disruptive effect of 5 mg/kg PCP at 15db above background compared to WT mice (*Brd1*$^{+/-}$ n=13, WT n=11) (t test, p<0.01). Data shown are mean and SEM for each group. *p<0.05 **p<0.01 ***p<0.001.

Figure 3

***Brd1*$^{+/-}$ mice are sensitive to the behavioral effects of psychotomimetics, show region-specific changes in tissue neurotransmitter levels, and altered striatal transcriptomic profile. (A)** PCP-induced hyperlocomotion is increased in *Brd1*$^{+/-}$ mice. Mice were placed in an observation box and allowed to acclimate, then injected with PCP and scored for activity as measured by number of infra-red beams crossed. *Brd1*$^{+/-}$ mice exhibited greater sensitivity to 5 mg/kg of PCP than WT mice (*Brd1*$^{+/-}$ n=12, WT n=12) (Two-way RMANOVA, effect of genotype, $F_{1,22}$=5.9, p<0.01). **(B)** Bar graphs show total accumulative activity during two hours of recording after PCP/vehicle injection. *Brd1*$^{+/-}$ mice exhibited greater sensitivity to 5 mg/kg of PCP than WT mice (*Brd1*$^{+/-}$ n=12, WT n=12) (t test, p<0.01). **(C)** *Brd1*$^{+/-}$ show altered hyperactivity response upon challenge with cocaine. Setup as described above for PCP (*Brd1*$^{+/-}$ n=12, WT n=12). Rather than responding with an increase in activity, *Brd1*$^{+/-}$ mice reach peak activity earlier than WT mice when administered 30 mg/kg of cocaine (Two-way RMANOVA, genotype x time interaction effect, $F_{23,506}$=2.043, p<0.01). **(D)** but shows no overall increased activity response to any dose of cocaine. **(E)** *Brd1*$^{+/-}$ mice respond with increased rearing activity compared to WT mice at a lowdose of cocaine (10 mg/kg) (t test, p<0.05). **(F)** Striatal DA level is elevated in *Brd1*$^{+/-}$ mice (n=11) compared to WT mice (n=10) (t test, p<0.05) whereas DOPAC and HVA levels are similar. **(G)** 5-HT tissue levels were significantly elevated in striatal tissue in *Brd1*$^{+/-}$ mice (n=14) compared to WT mice (n=16)(t test, p<0.05) **(H)** Western blotting analysis of protein extracts derived from tissue micro-punches from right striatum from WT and *Brd1*$^{+/-}$ mice (n=10 for each genotype). Top membrane was incubated with anti-Drd2 antibody and lower part of the membrane with anti-Hprt antibody. Densitometric analysis of relative protein amounts, normalized to the amounts of Hprt, showed an approximate 50% reduction in Drd2 protein in *Brd1*$^{+/-}$ mice compared to WT mice. Data shown are mean + SEM for each group. *p<0.05.

Figure 4

***Brd1*$^{+/-}$ mice show deficient GABAergic synaptic neurotransmission, transcriptomic changes, and reduced number of parvalbumin immunoreactive neurons in aCC. (A)** Mice were administered doses of 40, 55, or 70 mg/kg PTZ and observed for seizure activity for 30 min. and for tonic seizures for an additional 30 min. *Brd1*$^{+/-}$ mice (n=12) displayed significantly more jerks at 70 mg/kg PTZ than WT mice (n=12; *t* test with Welch's correction, $p<0.05$), whereas no difference was observed at low and intermediate doses. **(B)** Several mice went into seizures more than once when tested with 70 mg/kg. *Brd1*$^{+/-}$ mice (n=12) showed significantly more incidences than WT mice (n=12; Kruskal-Wallis test, $p<0.05$) 1st, 2nd, and 3rd refers to the order of seizure occurrence. **(C)** A tendency was noted with *Brd1*$^{+/-}$ mice going into clonic seizures earlier than WT mice regardless of dose. However, the difference was only significant for the lower dose (Peto-Peto-Prentice, $p<0.05$). When adjusting for dose effect, the overall significance level was also significant (Peto-Peto-Prentice, combined; $p<0.05$). **(D, E)** Whole-cell recordings of spontaneous inhibitory postsynaptic currents (sIPSCs) from exemplar aCC pyramidal neurons layer 2/3 in *Brd1*$^{+/-}$ and WT mice. **(F, G)** Whole-cell recordings of miniature inhibitory postsynaptic currents (mIPSCs) from exemplar aCC pyramidal neurons layer 2/3 in *Brd1*$^{+/-}$ and WT mice. In order to isolate mIPSCs, recordings were done in the presence of the Na^+ channel blocker tetrodotoxin (1 μM). **(H)** Averaged cumulative probability plot showing altered distribution of sIPSC inter-event intervals in aCC layer 2/3 pyramidal neurons of *Brd1*$^{+/-}$ mice (WT, black; *Brd1*$^{+/-}$, red) (Two-sample Kolmogorov-Smirnov test, $p<0.05$). Inset: *Brd1*$^{+/-}$ mice show lower mean frequency of sIPSCs in aCC pyramidal neurons layer 2/3 of *Brd1*$^{+/-}$ mice in comparison to WT mice (*Brd1*$^{+/-}$: 9.6 ± 1.6 Hz; n_{cells}=13; WT: 16.8 ± 2.1 Hz, n_{cells}=13) (*t* test, $p<0.05$). **(I)** Averaged cumulative probability plots showing altered distribution of mIPSC inter-event intervals in aCC layer 2/3 pyramidal neurons of *Brd1*$^{+/-}$ mice (WT, black; *Brd1*$^{+/-}$, red) (Two-sample Kolmogorov-Smirnov test, $p<0.05$). Inset: *Brd1*$^{+/-}$ mice

show lower mean frequency of mIPSCs in aCC pyramidal neurons layer 2/3 in comparison to WT mice (*Brd1*$^{+/-}$: 5.1 ± 0.6 Hz; n_{cells}=16; WT: 8.3 ± 0.7 Hz, n_{cells}=16) (*t* test, p<0.01). **(J)** Averaged cumulative probability plot showing distribution of sIPSC amplitudes in aCC layer 2/3 pyramidal neurons of *Brd1*$^{+/-}$ mice (WT, black; *Brd1*$^{+/-}$, red) (Kolmogorov-Smirnov test, p<0.05). Inset: mean sIPSCs amplitudes in aCC pyramidal neurons layer 2/3 were similar between *Brd1*$^{+/-}$ and WT mice (*Brd1*$^{+/-}$: 38.4 ± 2.2 pA, n_{cells}=13; WT: 43.6 ± 2.0 pA, n_{cells}=13). **(K)** Averaged cumulative probability plot showing similar distribution of mIPSC amplitudes in aCC layer 2/3 pyramidal neurons of *Brd1*$^{+/-}$ and WT mice (WT, black; *Brd1*$^{+/-}$, red). Inset: mean mIPSCs amplitudes in aCC pyramidal neurons layer 2/3 were similar between *Brd1*$^{+/-}$ and WT mice (*Brd1*$^{+/-}$: 34.5 ± 2.1 pA, n_{cells}=16; WT: 35.7 ± 1.7 pA, n_{cells}=16). **(L)** Reduced number of Pvalb labeled interneurons in aCC of *Brd1*$^{+/-}$ mice. Representative images of Pvalb expressing neurons in aCC (coronal sections) of WT and *Brd1*$^{+/-}$ mice (*top row*). Stereological estimation shows an approximate 28% reduction in the number of Pvalb-labeled interneurons in aCC of *Brd1*$^{+/-}$ mice (*bottom row*) (t test, p<0.05). cc; corpus callosum, L1; Cortical layer 1. *p<0.05, ***p<0.001 and n_{cells}=number of neurons tested. Data shown are mean and SEM for each group unless specifically stated otherwise.

Figure 5

Molecular changes converge in Dopamine-DARPP32-CREB signaling in *Brd1*$^{+/-}$ mice.

(A) Western blotting analysis of protein extracts derived from pulverized whole brains from WT (*n*=4) and *Brd1*$^{+/-}$ mice (*n*=5). Membrane was incubated with anti-CREB and anti-c-FOS antibodies, stripped and subsequently incubated with anti-phospho-CREB (Ser133) (pCREB) and tubulin antibodies. Densitometric analysis of relative pCreb/Creb protein amounts showed an approximate 40% increase in phosphorylated Creb protein in *Brd1*$^{+/-}$ mice compared to WT mice and c-Fos/Tubulin revealed an approximate 30% upregulation of c-Fos in *Brd1*$^{+/-}$ mice. Data shown are mean + SEM for each group. **p*<0.05. **(B)** DEGs, DEG enriched canonical pathways, and IPA predicted upstream regulators identified in the striatum of *Brd1*$^{+/-}$ mice converge in G-protein coupled receptors (GPCR)/cAMP/PKA/DARPP-32/CREB signaling in GABAergic medium-sized spiny neurons (MSNs), the predominant cell type of the striatum. In short: The DARPP-32 signaling pathway integrates information from a variety of neurotransmitters but mainly DA. In striatum, extracellular DA level is determined by a combination of mesolimbic DA activity and release probability at the synapse. Acetylcholine regulates the release probability through activation of nicotinic receptor heteromers containing α_6 or α_4 subunits and muscarinic receptor M_2 and M_4 (61). Through GPCRs, DA regulate the activity of adenylyl cyclase (AC) and thereby cAMP production. cAMP activates PKA which can activate DARPP-32 (71) or directly activate AMPA receptors and thereby control corticostriatal neurotransmission (72). Glutamate induces calcium influx through activation of AMPA and NMDA receptors which indirectly de-activates DARPP-32. Dependent on phosphorylation status, DARPP-32 may then, through indirect mechanisms, facilitate activation of CREB and thus transcriptional regulation of immediate early genes (IEG), glutamate receptors, and numerous downstream physiological effectors ultimately affecting synaptic plasticity. Red asterisks mark DEGs, components of DEG enriched canonical pathways, and IPA

predicted upstream regulators identified in striatum of *Brd1*$^{+/-}$ mice. For detailed description see **Figure S12**. Illustration adapted from Greengard et al. 1999 (73) and Berke et al. 2000 (74).

TABLES

Table 1 | Summary of behavioral analysis in *Brd1*$^{+/-}$ mice

Test Parameter measured	**Response**[1]	**Specific implication to schizophrenia**[2]	**Symptom domain**
Social interaction Passive interaction Latency to first interaction	 Decreased* Increased**	Asociality/social withdrawal	**Negative**
Three chamber sociability test Sociability Social recognition Remote social memory	 Decreased*** NC Decreased*	Asociality/social withdrawal Social cognition	
Spontaneous alternation -Basal -PCP	 NC Decreased*	Working memory	**Cognitive**
Continuous alternation -Basal -PCP	 NC Decreased**	Working memory	
Fear conditioning Conditioned learning Contextual memory -day 3 -day 4	 Decreased** Decreased** Decreased***	Associative learning / memory (long term memory)	
ASR -Basal -PCP -Amphetamine	 Increased* NC NC	Sensorimotor processing	**Cognitive/positive**
PPI -Basal -PCP -Amphetamine	 NC Decreased* NC	Sensorimotor gating / Pre-attentive processing	
Spontaneous- and drug-induced activity -Basal -PCP -Cocaine -Amphetamine	 NC Increased** Increased* NC	Psychomotor agitation / Drug sensitivity	**Positive**

1) *Brd1*$^{+/-}$ mice compared to WT littermates, 2) Possible relevance to the three symptom classes of schizophrenia (negative, cognitive, and positive). NC: No change. *p<0.05, **p<0.01, and ***p<0.001 in statistical tests between genotypes.

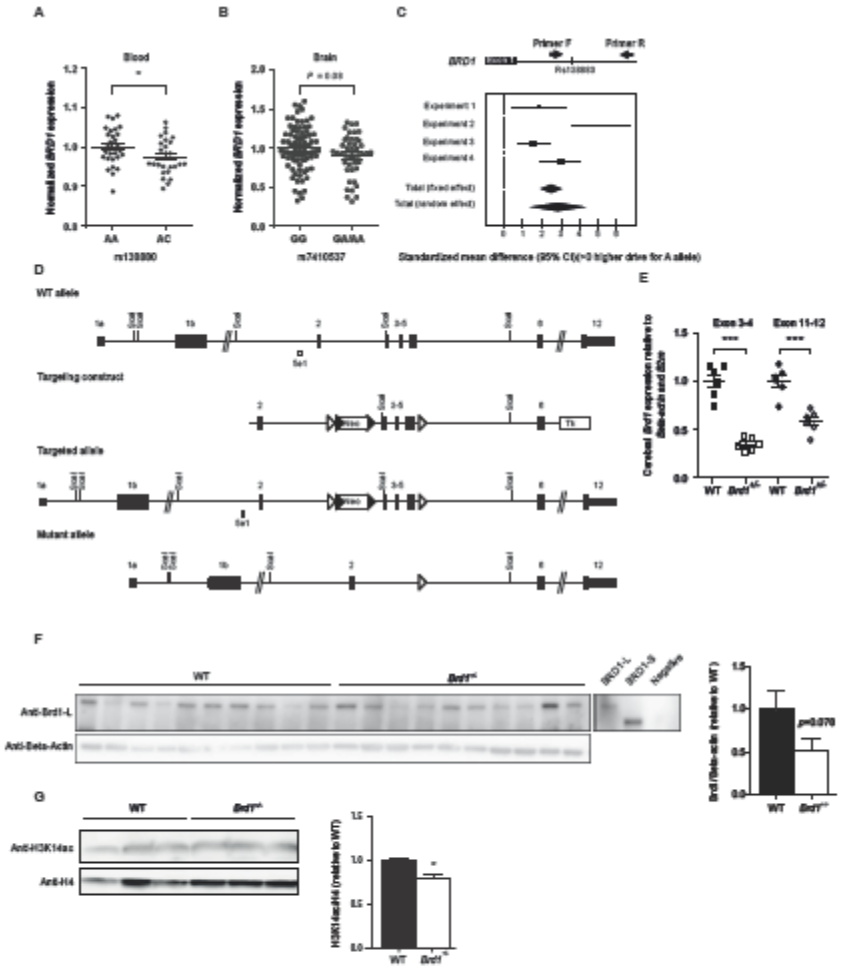
A
Blood
AA
AC
rs139890
B
Brain
GG
GAMA
rs7410537
C
Primer F
Primer R
Experiment 1
Experiment 2
Experiment 3
Experiment 4
Total (fixed effect)
Total (random effect)
Standardized mean difference (95% CI)(>0 higher drive for A allele)
D
WT allele
Targeting construct
Targeted allele
Mutant allele
E
Exon 3-4
Exon 11-12
WT
Brd1AC
F
WT
Brd1AC
Anti-Brd1-L
Anti-Beta-Actin
p=0.070
G
Anti-H3K14ac
Anti-H4

Qvist et al.

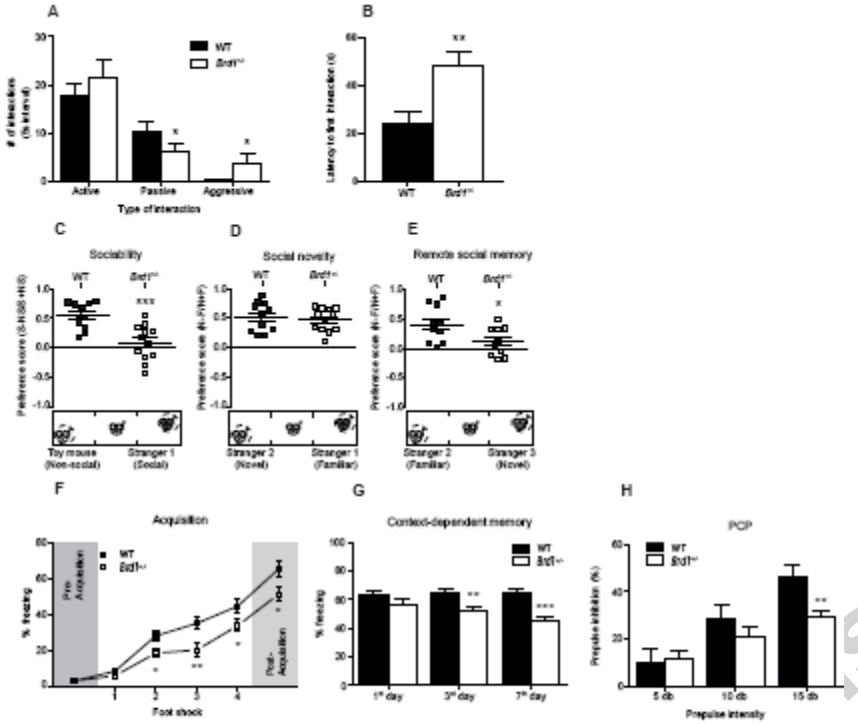
A
B
C
D
E
F
G
H
WT
Active
Passive
Aggressive
Type of interaction
Sociability
Social novelty
Remote social memory
Toy mouse (Non-social)
Stranger 1 (Social)
Stranger 2 (Novel)
Stranger 1 (Familiar)
Stranger 2 (Familiar)
Stranger 3 (Novel)
Acquisition
Pre-Acquisition
Post-Acquisition
Foot shock
Context-dependent memory
1st day
3rd day
7th day
PCP
5 db
10 db
15 db
Prepulse intensity

Qvist et al.

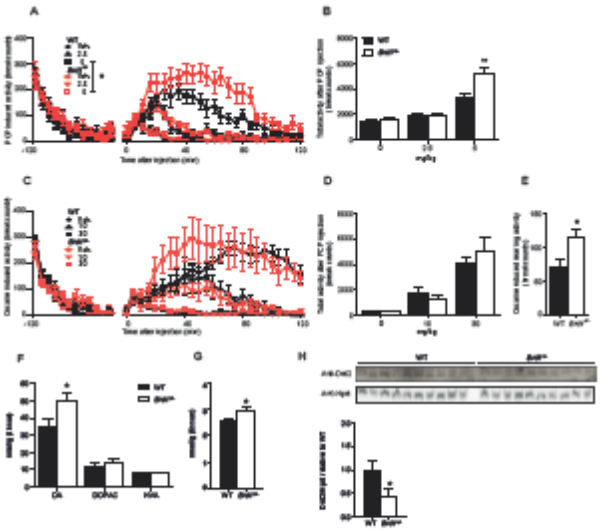

Qvist et al.

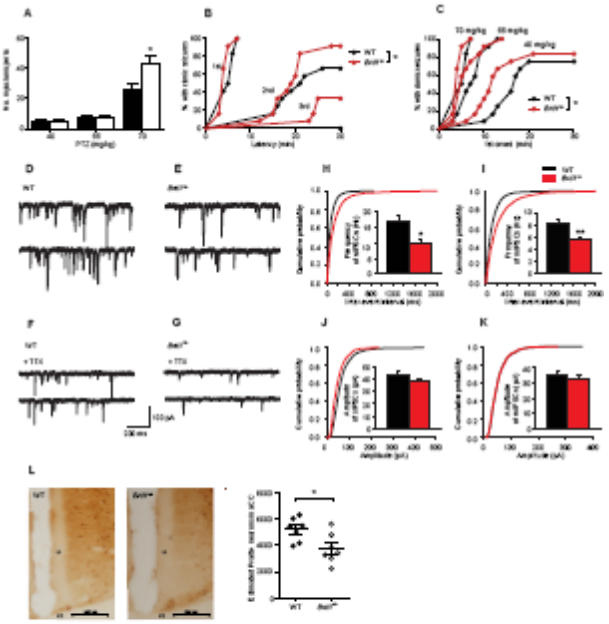

Qvist et al.

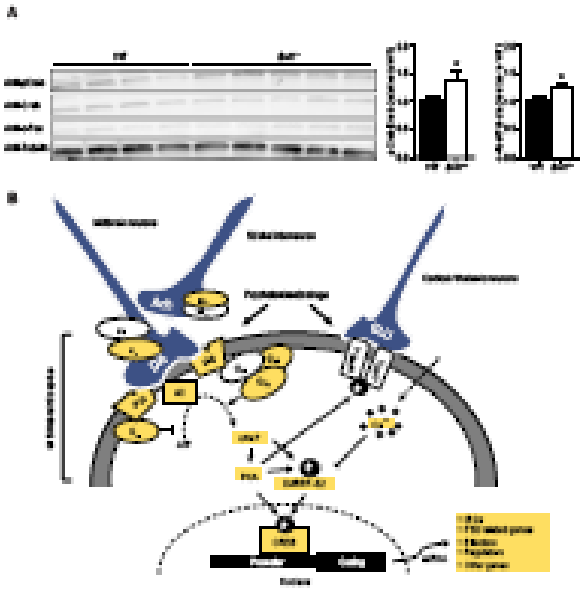

Qvist et al.